Proceedings of the Institute of Acoustics & Belgium Acoustical Society
Noise in the Built Environment, Ghent, 29-30 April 2010

THE USE OF STATISTICAL ENERGY ANALYSIS (SEA) FOR THE PREDICTION OF THE SOUND REDUCTION INDEX OF DOUBLE SYSTEMS WITH LARGE CAVITY

M Blasco BLASCO Ltd, Merksem, Belgium
G Vermeir K.U.Leuven, Leuven, Belgium
A De Herde U.C.Louvain, Louvain-La-Neuve, Belgium

Over the last ten years, a high amount of (high-rise) double façades buildings, consisting of two façades with glass and aluminum separated by a large cavity, have been built. The usefulness of acoustic prediction models has become evident, especially at the tendering phase of a project. A double façade combines mostly a double glazing with a single glazing, yielding three different glass panes in the system (figures 1 and 2).
Statistical energy analysis (SEA) will be used in this paper to study the transmission of diffuse-incidence sound waves through a double system consisting of two independent glass panels, separated by a large air space. The analytical SEA model consists of seven linearly coupled subsystems. Both non-resonant and resonant transmissions for the glass panels are included. The prediction using SEA was compared to the acoustic measurements, which were conducted for this study at the Catholic University of Leuven in Belgium (K.U.Leuven), of sixteen different double façade systems. The agreement with the experimental data revealed to be good to very good.

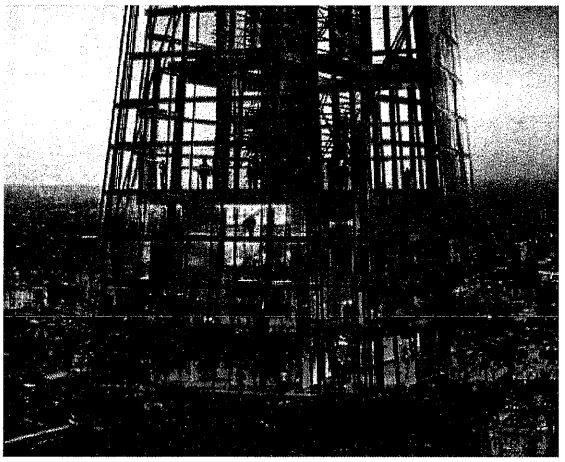

Fig.1 - External view of a double façade
Project "The Shard" – Arch. R. Piano

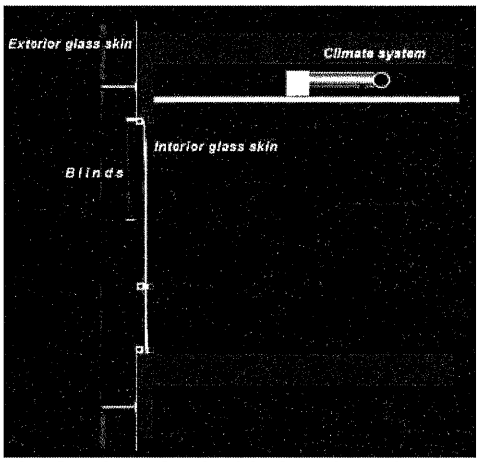

Fig.2 - Section of a double façade, using a total of three glass panes (one on the exterior skin and two on the interior skin)

LIST OF SYMBOLS

c_L	Speed of longitudinal panel waves (m/s)
d	Cavity depth (m)
f	Frequency (Hz)
f_c	Critical frequency (Hz)
f_d	First cross cavity mode frequency (crossover frequency) (Hz)
h	Plate thickness (m)
k	Wavenumber (radians/m)
k_B	Bending wavenumber (radians/m)
k_m	Bending wavenumber of mth panel mode
m	Mass (kg)
m"	Surface mass (kg/m²)
n(f)	Modal density (modes per Hz)
n(ω)	Modal density (modes per radians/s)
ρ	Sound pressure (Pa)
s	Standard deviation
t	Time (s)
w	Energy density (J/m^3)
A	Absorption area (m^2)
E_i	Total (modal) energy of system i (J)
$L_{x,c}$	Dimension of the cavity measured according to dimension x (m)
$L_{y,c}$	Dimension of the cavity measured according to dimension y (m)
R	Sound reduction index (dB) – see also SRI
R_w	Single value of the SRI according to EN ISO 717-1(1996) (dB)
S	Surface (m²)
SPL	Sound pressure level (dB)
SRI	Sound reduction index (dB) – see also R
V	Volume (m^3)
W_{ij}	Power flow from system i to j (Watt)
W_i^{diss}	Power dissipated internally by system i (Watt)
W_i^{in}	Power supplied to system i (Watt)
Z_0	Characteristic impedance of air (Pa.s/m)
Z_p	Surface impedance of a plate (Pa.s/m)
α_0	Normal incidence sound absorption coefficient (-)
η	Loss factor (-)
η_{int}	Internal loss factor (-)
η_{rad}	Loss factor due to acoustic radiation (-)
η_{edge}	Loss factor due to structural coupling at the boundaries (-)
η_i	Internal loss factor for subsystem i (-)
η_{ij}	Coupling loss factor from subsystem i to subsystem j (-)
η_{total}	Total loss factor (-)
κ	Gas compressibility (Pa^{-1})
λ	Wavelength (m)
ν	Poisson's ratio (-)
ρ	Density (kg/m^3)
σ	Radiation efficiency (-)
σ_{rad}	Radiation ratio (radiation resistance) = Sρcσ
ω	Angular frequency ω = 2πf (radians/s), angular velocity (radians/s)
< >	space-time average

1 INTRODUCTION

Statistical Energy Analysis (SEA) [9] is a method for predicting vibration transmission in dynamical systems made of coupled acoustic cavities and structural parts. The vibrational behaviour of the system is described in the energy domain. The energy is here the potential and kinetic energy carried out by the modal resonances of the dynamical system. To solve a problem with SEA, the system must be partitioned into "subsystems", i.e. regions of the system where energy is equally shared among modes. SEA then consists in writing a set of power-balanced equations that couples the power injected by the external loads (the sources) and the energies of the various subsystems. The successful prediction of noise and vibration levels depends largely on an accurate estimation of three parameters, being the modal densities and the internal loss factors of individual subsystems and the coupling loss factors between the subsystems.
The SEA formulae are confined to systems where the average mean square velocities are determined by the amplitudes of resonant modes. Accordingly, the SEA considers only the free vibrations not the forced ones.
The procedures of SEA can be thought of as the modeling of elastic mechanical systems and fluid systems by subsystems, each one comprising groups of multiple oscillators, with a probabilistic description of the relevant system parameters. The analysis is thus about the subsequent energy flow between the different groups of oscillators.
The procedures are based upon several general assumptions, namely:
there is a linear, conservative coupling (elastic, inertial and gyrostatic) between the different subsystems; the energy flow is between the oscillator groups having resonant frequencies in the frequency bands of interest; the oscillators are excited by broadband random excitations with uncorrelated forces (i.e. not point excitation) which are statistically independent – hence there is modal incoherency, and this allows for a linear summation of energies; there is equipartition of energy between all the resonant modes within a given frequency band in a given subsystem; the principle of reciprocity applies between the different subsystems; the flow of energy between any two subsystems is proportional to the actual energy difference between the coupled subsystems whilst oscillating – i.e. the flow of energy is proportional to the difference between the average coupled modal energies.
SEA is most successful (i) when there is a weak coupling between subsystems; (ii) when the exciting forces are broadband in nature; (iii) when the modal densities of the respective subsystems are high; and (iv) when the assumptions outlined before are fulfilled.
SEA procedures can still be used in practice if any of the preceding criteria are not strictly met. The results are generally not as reliable as they otherwise might be, but they can provide a qualitative assessment of the problem.
If the coupling loss factors are much smaller than the internal loss factor and structural loss factor, we have "weak couplings" which is a requirement to apply the SEA models. When this is the case, there is no indirect coupling and the coupled and uncoupled modal energies are approximately equal. Indirect coupling indicates that the energy flow between two groups of oscillators is influenced by other oscillator groups in the overall system; so energy terms between oscillators which are not directly coupled have to be accounted for.
Price & Crocker [12] compared the use of SEA with systems consisting of two panels separated by an absorbing cavity. They obtained good agreement with experimental results.
For more detailed information on SEA we refer to specialised literature.

2 ANALYSIS

2.1 The Use of a (steady-state) SEA Model using seven coupled subsystems

In this paper we use SEA to study the transmission of random-incidence sound waves through three (parallel) glass panels separated by an air cavity, representing a double façade system [10]. This sound transmission problem can be considered as a seven-coupled-oscillator system, arranged room-panel-cavity-panel-large cavity-panel-room (figure 3). In the continuation of this paper it will be studied in this manner.

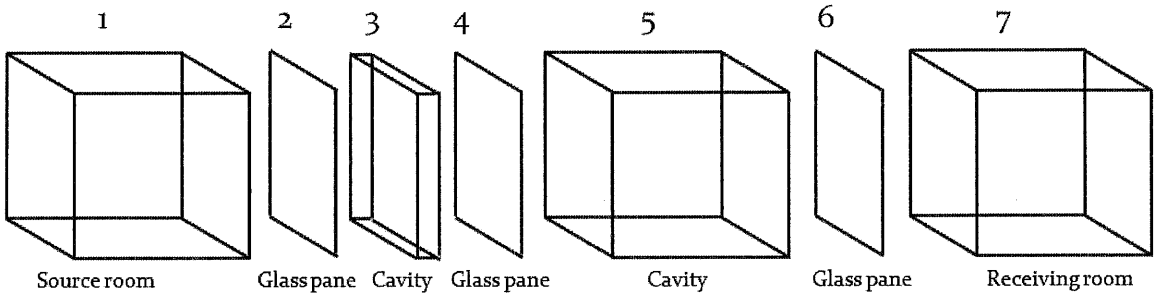

Figure 3: Arrangement of rooms, panes and cavities representing a double façade system

If a set of oscillators is linearly coupled, then the power flow W_{ab} from one system to another is directly proportional to the difference of the modal energies of the system [12]:

$$W_{ab} = \phi_{ab} (<E_a> - <E_b>)$$

ϕ_{ab} being the coupling factor

We consider a transmission suite in which a pair of structurally isolated reverberant rooms is acoustically connected by three parallel panels, each panel being fixed with clamped edges, in an aperture, in adjacent walls of each room. The cavities are empty. This analytical model may be considered to consist of seven coupled resonant systems, as shown in figure 4. The power-flow balance equations give:

$$W_1^{in} = W_1^{diss} + W_{12} + W_{13}$$
$$W_2^{in} = W_2^{diss} + W_{23} + W_{24} - W_{12} = 0$$
$$W_3^{in} = W_3^{diss} + W_{34} + W_{35} - W_{13} - W_{23} = 0$$
$$W_4^{in} = W_4^{diss} + W_{45} - W_{24} - W_{34} = 0$$
$$W_5^{in} = W_5^{diss} + W_{56} + W_{57} - W_{35} - W_{45} = 0$$
$$W_6^{in} = W_6^{diss} + W_{67} - W_{56} = 0$$
$$W_7^{in} = W_7^{diss} - W_{57} - W_{67} = 0$$

We only have power input in the sending room, through the loudspeaker, so $W_1^{in} <> 0$, all other power inputs are equal to zero (Figure 4).

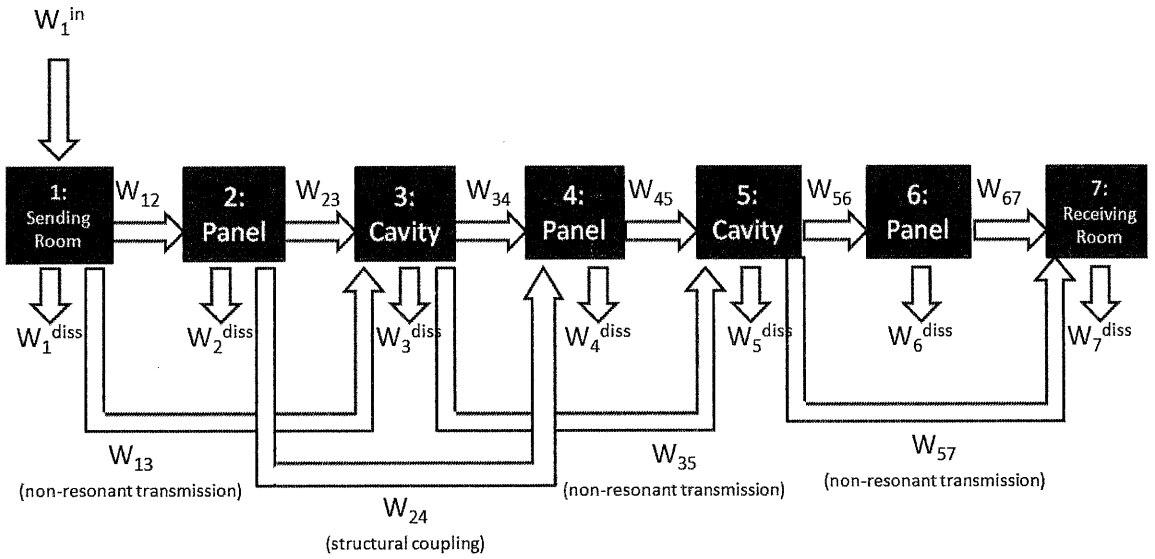

Figure 4: Block diagram representing power flow in the seven coupled oscillator system

2.2 Calculation of a seven coupled oscillator (steady-state) SEA model

Following equations from paragraph 2.1, and [4, 9, 14]:

$$W_i^{in} = \omega \eta_i E_i$$
$$W_{ij} = \omega \eta_{ij} n_i (E_i/n_i - E_j/n_j)$$

We obtain:

$$E_1/E_7 = f(\eta_{ij}, \eta_{jt})$$

With: i=1,...,7 and j=2,...,7

where η_i is the loss factor of system i, and η_{ij} is the coupling loss factor from system i to system j. The relation between the modal energies and the SRI is given by [9, 12]:

$$SRI = 10log\frac{E_1}{E_7} - 10log\frac{V_1}{V_7} + 10log\frac{ScT_7}{24V_7 ln10}$$

(1: source room, 2: first panel, 3: cavity, 4: second panel, 5: cavity, 6: third panel, 7: receiving room).
Where E_i is the total (modal) energy of system i, V_i is the volume of system i, and T_i is the reverberation time system i.

2.3 Evaluation of the parameters

The double façade modeled consists of three finite parallel panes separating two finite volumes with diffuse field conditions (reverberant field would be more correct). All panes are isotropic and homogeneous, without openings or slits. All panes have finite dimensions, a mass, a loss factor and a finite bending stiffness. Both resonant and non-resonant transmissions for the panels are considered under diffuse incidence. The sound reduction index is strongly dependent upon the radiation resistance of the panels, the panel and cavity loss factors and the panel spacing, as will be seen. The radiation resistance is based on Maidanik's model [8]. The spring property of the air in the cavity is ignored. Instead of using the mass-spring-mass resonance, we divide the sound field in the cavity into low-order modes (wavelength > d/2) and high-order modes (wavelength < d/2).
The empty cavity is considered as a resonant system in which the modal density and loss factor are determined analytically. According to Brekke [2], when dealing with reflecting edges in the cavity, an appropriate normal incidence absorption coefficient can be used. In his study, Brekke derived empirical absorption coefficients, which will be used in this paper.

2.3.1 Coupling loss factors

The use of coupling loss factors (volume-plate, volume-volume) is crucial in SEA models. The total loss factor (steady-state condition) of a subsystem is calculated as the sum of its internal loss factor and all coupling loss factors for that subsystem. The internal loss factor is obtained from a structural reverberation time measurement (EN ISO 140-3 (1995) annex E [17]).

2.3.1.1 PANEL-ROOM

The modal density of a simply supported panel is:

$$n_p(\omega) = \frac{\sqrt{3}S}{2\pi h c_L} \quad [\frac{modes}{rad.s}]$$

Where:
h: thickness panel [m]
S: surface panel [m²]
Longitudinal wave speed: $c_L=\sqrt{(B/\rho)}$ = 5430 m/s (for glass)
The formula is valid for any boundary condition at high frequencies. At low frequencies the formula is not valid. If we look at the modal density of the room,

$$n_R(\omega) = \frac{V\omega}{2\pi^2 c^3} \quad [\frac{modes}{rad.s}]$$

then using the consistency relationship (SEA) [4, 9] we yield (1: room, 2: panel):

$$\eta_{12} = \frac{\eta_{21}.n_2}{n_1} = \frac{\sigma_{rad,2}}{\omega M_2}.\frac{\sqrt{3}S}{2\pi h c_L}.\frac{2\pi^2 c^3}{V\omega^2} = \frac{\sigma_{rad,2}\sqrt{3}S\pi c^3}{\omega^3 M_2 h c_L V}$$

Where:
M_i: total mass of subsystem i
$\sigma_{rad,i}$: radiation factor of subsystem i
An analogue calculation is done for η_{67}.

2.3.1.2 PANEL-CAVITY

The equations for the coupling loss factors will depend on either the frequency is bigger or smaller than the critical frequency f_c of the panel. For this analysis the type of modes in the panels are crucial. There are corner, edge and surface modes. These have respectively increasing order of radiation efficiency (figure 5).
Resonant modes below the critical frequency are called "acoustically slow". These are subsonic modes ($c_m < c$ or $k_m > k$). The subsonic resonant modes can be subdivided into the corner modes (k_{mx}, $k_{ny} > k$) and edge modes ($k_{mx} > k$ or $k_{ny} > k$). Edge modes are more efficient radiators than corner modes (bigger surface); radiation from corner modes may be neglected. So for subcritical frequencies the resonant modes radiate through edge modes.

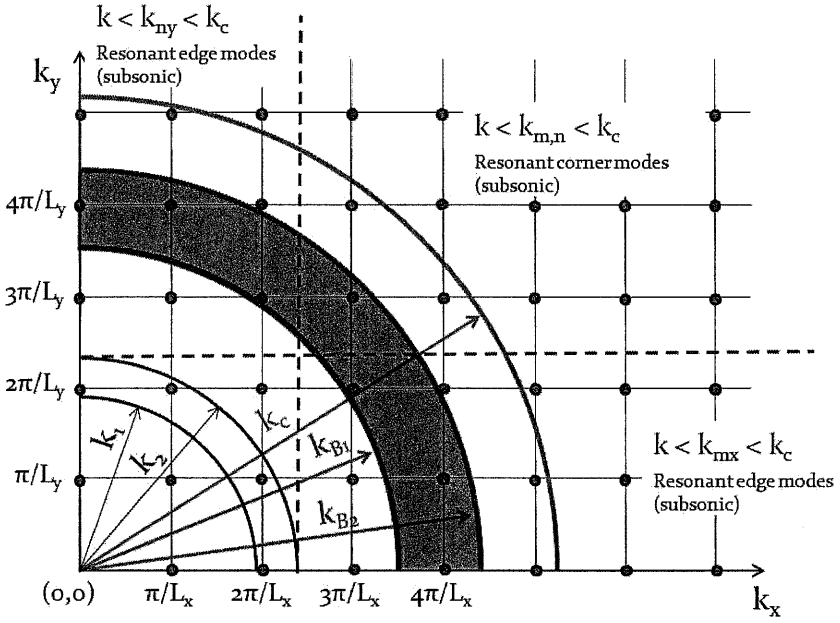

Figure 5: Corner and edge modes in k-space

In our measurement set-up, the edge modes do not radiate to half-space, but to a quarter space (due to the enclosed cavity, Figure 6). Therefore the radiation ratio will be two times bigger, yielding [12]:

$$\eta_{23} = \frac{2\sigma_{rad,2}}{\omega M_2} \qquad f < f_{c,2}$$

$$\eta_{43} = \frac{2\sigma_{rad,4}}{\omega M_4} \qquad f < f_{c,4}$$

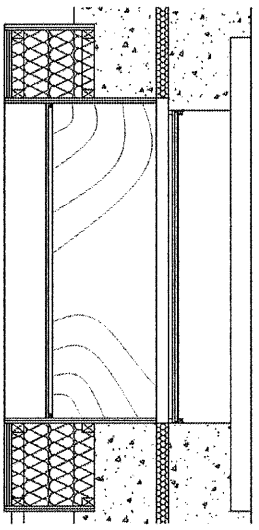

Figure 6: Radiation of the edge modes of the plate into the cavity of the double façade system

Resonant modes above the critical frequency are called acoustically fast ($c_m > c$ or $k_{mx} < k$). These radiate under the shape of surface *modes* and are very efficient; there is no cancellation of their

volume velocity and radiation is possible from their entire surface. These radiate into half-space [12]:

$$\eta_{23} = \frac{\sigma_{rad,2}}{\omega M_2} \qquad f > f_{c,2}$$

$$\eta_{43} = \frac{\sigma_{rad,4}}{\omega M_4} \qquad f > f_{c,4}$$

We have analogue calculations for η_{45} and η_{65}.

2.3.2 Loss factor of the cavity

The loss factor of the cavity depends on the frequency band of interest.
We have [12]:

$$\eta_i = \frac{Sc\alpha_0}{4V\omega} \qquad f < f_d \quad i = 3{,}5$$

$$\eta_i = \frac{Sc\alpha_0}{6V\omega} \qquad f > f_d \quad i = 3{,}5$$

Where V is the volume of the cavity [m³] , f_d is the crossover or first cross mode frequency, α_0 is the normal incident absorption coefficient and S is the total surface area of the absorbent in the cavity (understood as perimetrical absorption).
According to Brekke [5], the normal incident absorption can be evaluated as follows for empty cavities:
For cavity depths > 0.1 m, we have 10 log α_0 = -10 dB
For cavity depths < 0.02 m, we have 10 log α_0 = -3 dB

Interpolation may be used for intermediate values of the cavity depth.
The measurement of the reverberation time of the cavity of a double façade, allowed verification of these empirical values.

2.3.3 Radiation factor

The formulas for the radiation factor σ are taken from EN 12354-1, annex B [16].

2.3.4 Modal density of the cavity

To evaluate the modal density of the cavity we need to take different equations according to the frequency observed. To a good approximation we may use [Price &Crocker ,12]:

$$n_i = \frac{S_c\omega}{2\pi c^2} \qquad f < f_d \quad i = 3{,}5$$

$$n_i = \frac{V_i\omega^2}{2\pi^2 c^2} \qquad f > f_d \quad i = 3{,}5$$

The loss factors in the air cavity can be calculated from:

$$\eta_i = \frac{S_{c,a} c \alpha_0}{4 V_i \omega} \quad f < f_d \quad i = 3,5$$

$$\eta_i = \frac{S_{c,a} c \alpha_0}{6 V_i \omega} \quad f > f_d \, , i = 3,5$$

where S_c is the area of the cavity (m^2), and $S_{c,a}$ is the area of the absorbent in the boundaries of the cavity, being:

$$S_c = L_{x,c} L_{y,c}$$
$$S_{c,a} = 2d(L_{x,c} + L_{y,c}).$$

2.4 Non-resonant transmission

In a given frequency band, we encounter two types of modes: the resonant modes, with their natural frequency in the considered frequency band, and the non-resonant modes, with such an excitation that their natural frequencies fall outside the frequency band. These non-resonant modes are responsible for the "mass-law" transmission of sound. According to Price & Crocker [12], the value of transmission loss resulting from the non-resonant transmission in the system, should be expected to be the upper bound on the best insulation that can be obtained from the double façade, when neglecting the resonant transmission. If the damping would be increased in the system, the resonant transmission would become lower, leading to a sound insulation as calculated from the non-resonant transmission, particularly in the coincidence region.

3 EXPERIMENTS

In the experimental set-up we mounted several types of double façade systems, changing the thickness of the glass panes and the cavity depth. We compared the results of 16 measurements with the calculations using the SEA model as described before.
In the experiments, glass panes 2 and 4 are part of a double glazing with small cavity (12 to 15 mm) comprising a metallic spacer. The structural coupling between systems 2 and 4 is taken into account by the use of a total loss factor which was measured on the mounted double glazing in the aperture, in order to avoid the modeling of the structural coupling into a sub-system (metallic spacer). Literature states that the modeling of a structural coupling would be very difficult and agreement with measurement results would likely not work [Brekke ,2] [Hopkins ,6].

3.1 Experimental set-up

In figure 7, the measured double façades are schematically shown. The double façade consists of two façades, one being a single glazing and the other being a double glazing. The laboratory measurements were conducted at the Catholic University of Leuven in Belgium (K.U.Leuven).

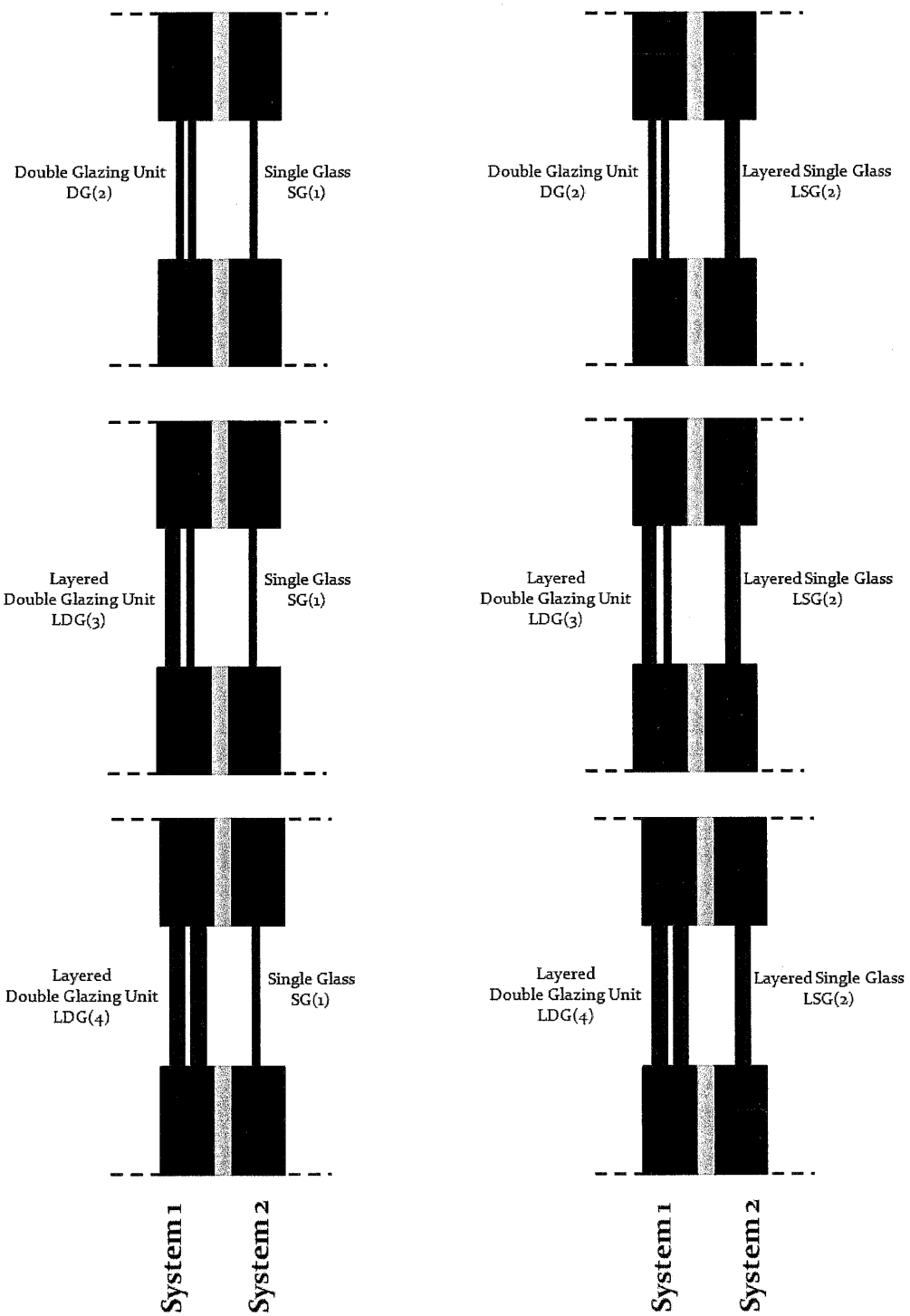

Figure 7: Schematic overview of the measured double façade systems in the laboratory

The types of glass panes used in the measured double façades are those which are most commonly used in the practice of office buildings [1]. This also means that one of the two façades is composed of a double glazing. A test matrix was set-up for small scale tests (according to EN ISO

140-3: 1995 [17]). The cavity depth was either 600 mm, 300 mm or 150 mm. For comparison with the SEA model we focused on closed systems (no opening or slits) without a metallic profile and without absorption in the cavity. Each façade of the double façade system was mounted on structurally uncoupled walls, eliminating any flanking path between the two façades (figure 8, figure 9). The façades have standardized dimensions of 1.23 m x 1.48 m. The sending and receiving rooms have volumes of 88 m³.

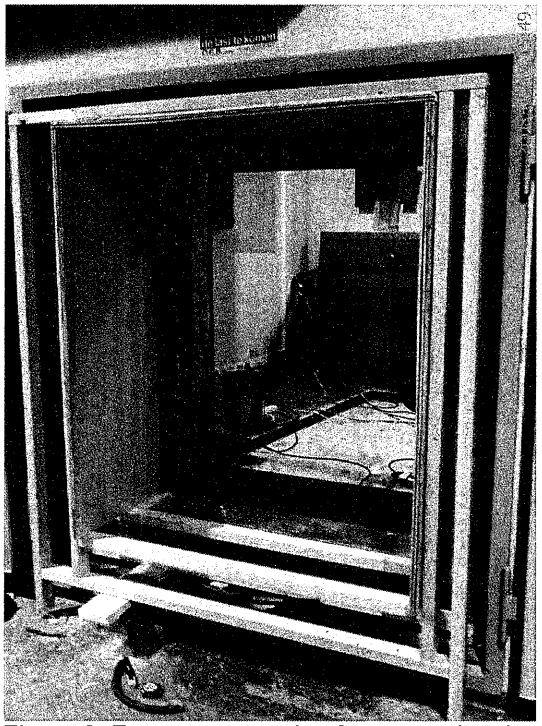

Figure 8: Frame construction for supporting the outer glass plate for big cavities

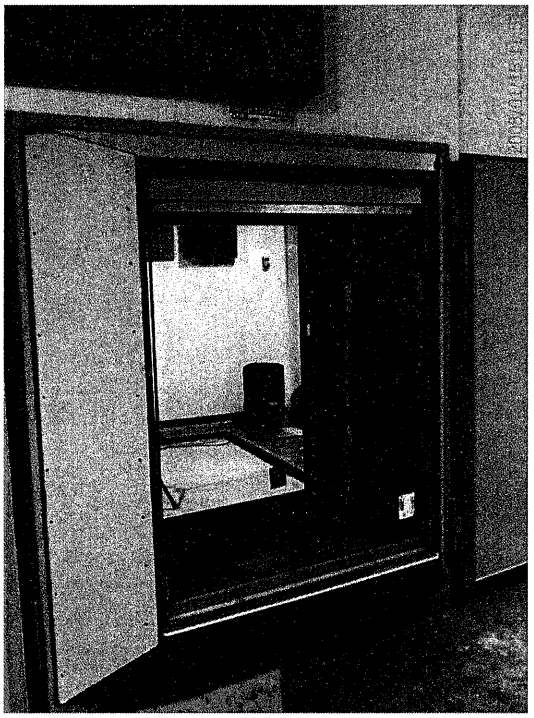

Figure 9: Finished double glass façade with cavity of 600 mm

Table 1 shows an overview of the for this study relevant double façade systems, with their measured single values of the SRI.

Table 1: Single value of the SRI $R_w(C;C_{tr})$ in decibels for different double façade systems

Single glass / Double glass	-	6 mm d=150 mm	6 mm d=300 mm	6 mm d=600 mm	1212.2 d=150 mm	1212.2 d=300 mm	1212.2 d=600 mm
6-12-8	35(-1;-4)	54(-2;-7)	58(-2;-5)	58(-2;-4)	59(-2;-6)	64(-1;-6)	66(-2;-6)
6-12-8 P.A.(4)	-	-	59(-3;-10)	-	-	-	-
8-16-44.2	38(-2;-6)	55(-2;-9)	59(-2;-7)	61(-2;-5)	58(-2;-7)	66(-2;-7)	67(-1;-6)
8-16-44.2 A(80%)	-	60(-2;-9)	-	-	-	-	-
10-18-66.2A	45(-1;-4)	59(-3;-9)	65(-3;-8)	66(-2;-7)	62(-3;-8)	69(-2;-8)	69(-2;-7)
66.2A-16-66.2A	49(-1;-6)	-	66(-3;-9)	68(-3;-8)	-	69(-2;-8)	69(-2;-7)
6 mm*	31(-2;-3)	-	-	-	-	-	-
10 mm*	34(-1;-3)	-	-	-	-	62(-1;-5)	63(-2;-5)
10 mm* P.A.(2)	-	-	-	-	-	65(-1;-6)	-
1212.2*	41(-1;-4)	-	-	-	-	-	-

*These systems are single glazings
A(80%): 80 % of cavity is filled with Rockwool
P.A.(2): Perimetrical absorption - 2 faces covered with 20 mm Rockwool
P.A.(4): Perimetrical absorption – 4 faces covered with 20 mm Rockwool

3.2 Measurement of the total loss factor of the double glazing

The main goal of this measurement was to avoid modeling the metallic spacer of the double glazing into a subsystem. The total loss factor was derived from the structural reverberation time (EN ISO 140-3 annex E) (Figure 11) [17] of both glass panes of a double glazing, different single glazings and a laminated single glazing. The impulse-response measurement was performed using hammer excitation. Two accelerometers were used for three excitation positions and two mean values. The procedure was repeated twice, resulting in a total of 24 measurements. The processing was based on the "Integrated Impulse Response Method" as described in ISO 3382 [18].

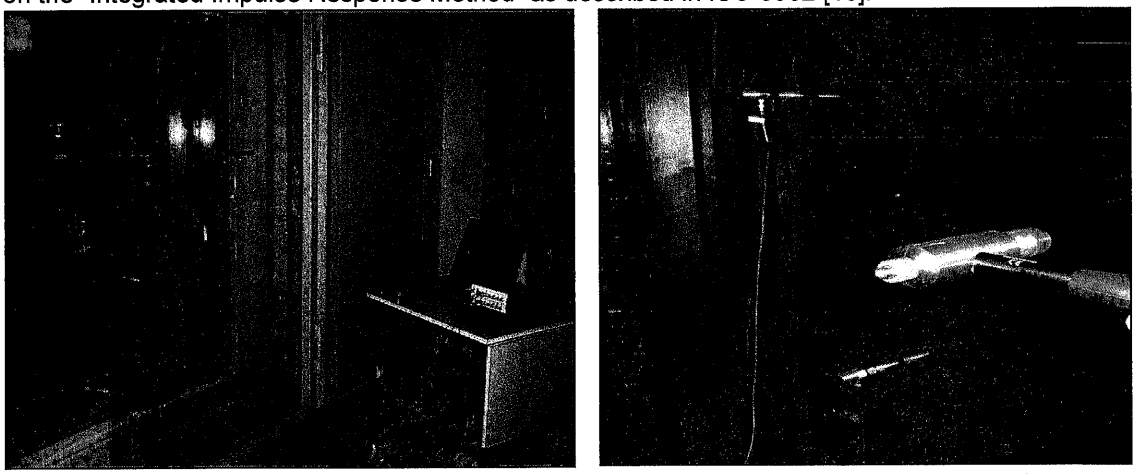

Figure 10: loss factor measurement set-up and close up of the accelerometer and impact hammer with rubber pad

The subsystem, being the acoustic room volume behind the measured sample enters a power balance equation. Measuring the loss factor in such conditions (in contrary to "in vacuum" which would be the appropriate way to measure the internal loss factor), replicates the conditions in which the double façades are measured. It is in fact a measurement of the total loss factor of the system being the glass panel and the acoustic volume behind it. This means that the measured loss factor also takes into account the room volume's internal loss factor. The room volume's internal loss factor is at least a factor 10 smaller than the measured loss factor, leading to negligible measuring errors. Also the coupling loss factors are 10 to 100 times smaller than the measured loss factor. We can then assume that the measured total loss factor is a good estimate of the internal loss factor (considering that the coupling loss factor due to structural connections are negligible), which will be used in the SEA model. When the measurement results do not vary significantly with frequency, an average loss factor can be determined for a chosen frequency range below the critical frequency (Figure 11).

Figure 11: Measurement of the total loss factor on 2 glass samples. the asterisk indicates which glass plate is impacted with the hammer.

In table 2 we find the single values of the measured loss factors for mounted panes. These values are used in the SEA model as they represent the conditions of mounting and the characteristics of the panel, used during the measurement of the SRI. These values take into account the internal properties of the panel (internal losses), the acoustic radiation (radiation losses) and the energy dissipation at the boundaries (edge losses). Using the average value of the measured loss factor in comparison to the spectral values, negligible differences were found in the prediction of the SRI (lower than 2 dB). The differences were the highest at and above the critical frequency.

Table 2: Average values of the measured loss factors for mounted panes					
Single glazing		**Double glazing**		**Laminated glass**	
pane	**η**	**pane**	**η**	**pane**	**η**
6	0.042	6	0.022	1212.2	0.054
8	0.047	8	0.027		
10	0.05				

3.3 Comparison SEA model and experimental results

The measured and theoretical transmission loss for the double façade systems appear to be in good agreement throughout most of the frequency range (figures 12, 13, 14, 15). Using a laminated single glazing in the system (e.g. 1212.2), the agreement is less good. For laminated glazings we calculated the critical frequency for thicknesses between the total thickness of the laminated glazing and the composing pane (i.e. for thicknesses 24 mm and 12 mm for 1212.2). This resulted in a better approximation with the measurements.
When measuring laminated double glazings, the laminated glazing gave a shift of 30% upwards with regards to the critical frequency. This observation was introduced in the model by multiplying the critical frequency of this type of glazing with an empirical factor of 1.3. The highest critical frequency of the laminated double glazing, corresponding with the thinnest glass pane, is generally not visible on the SRI curve.
The impact of different foils used for laminating the glass panes at the critical frequency, was evaluated empirically.

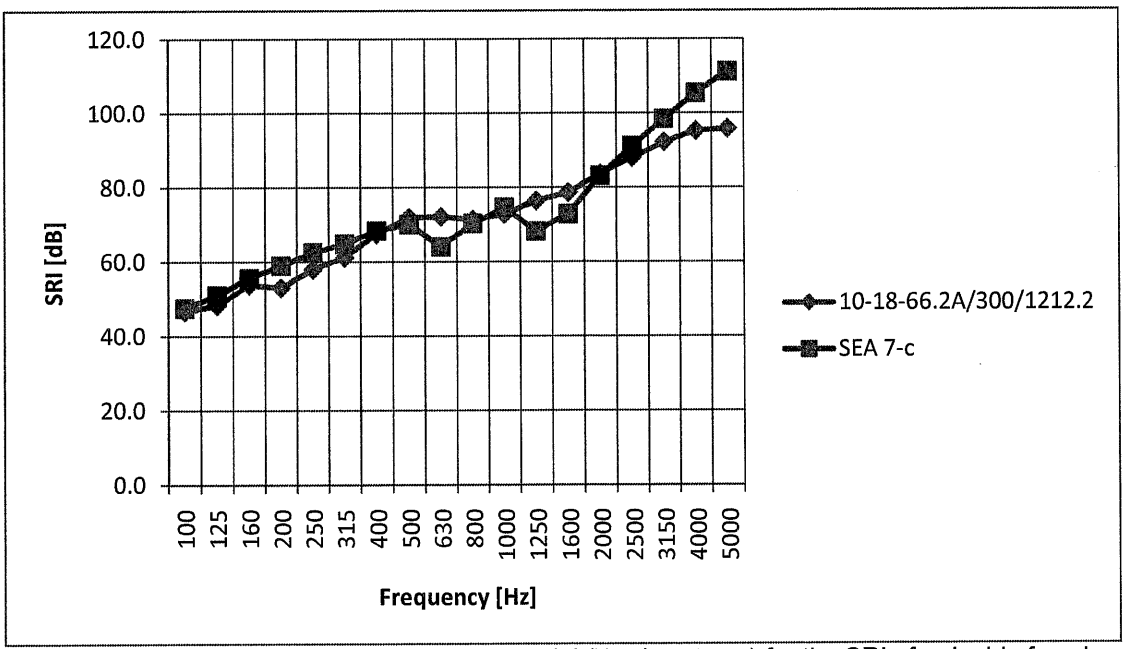

Figure 12: Comparison of the studied SEA model (7 subsystems) for the SRI of a double façade system with experimental result

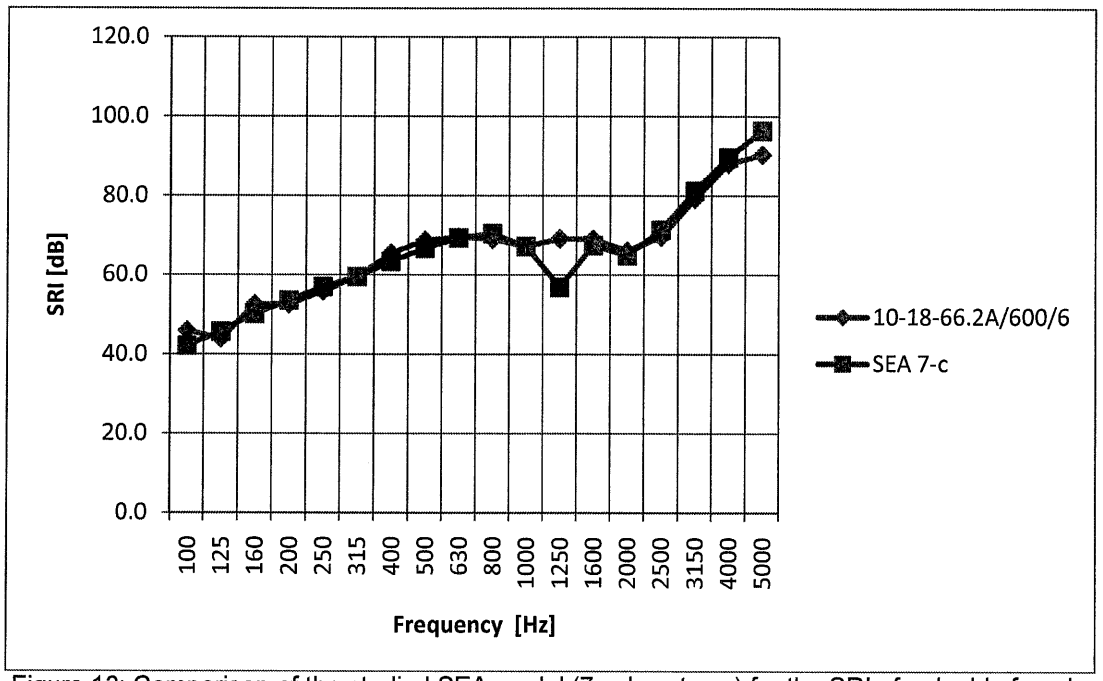

Figure 13: Comparison of the studied SEA model (7 subsystems) for the SRI of a double façade system with experimental result

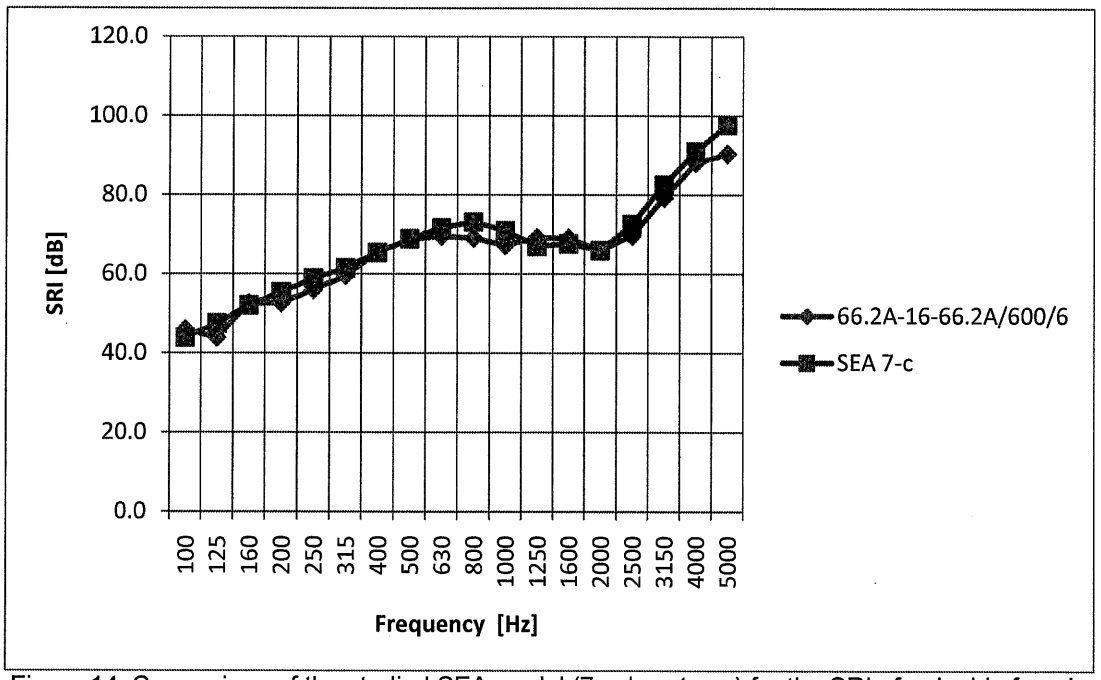

Figure 14: Comparison of the studied SEA model (7 subsystems) for the SRI of a double façade system with experimental result

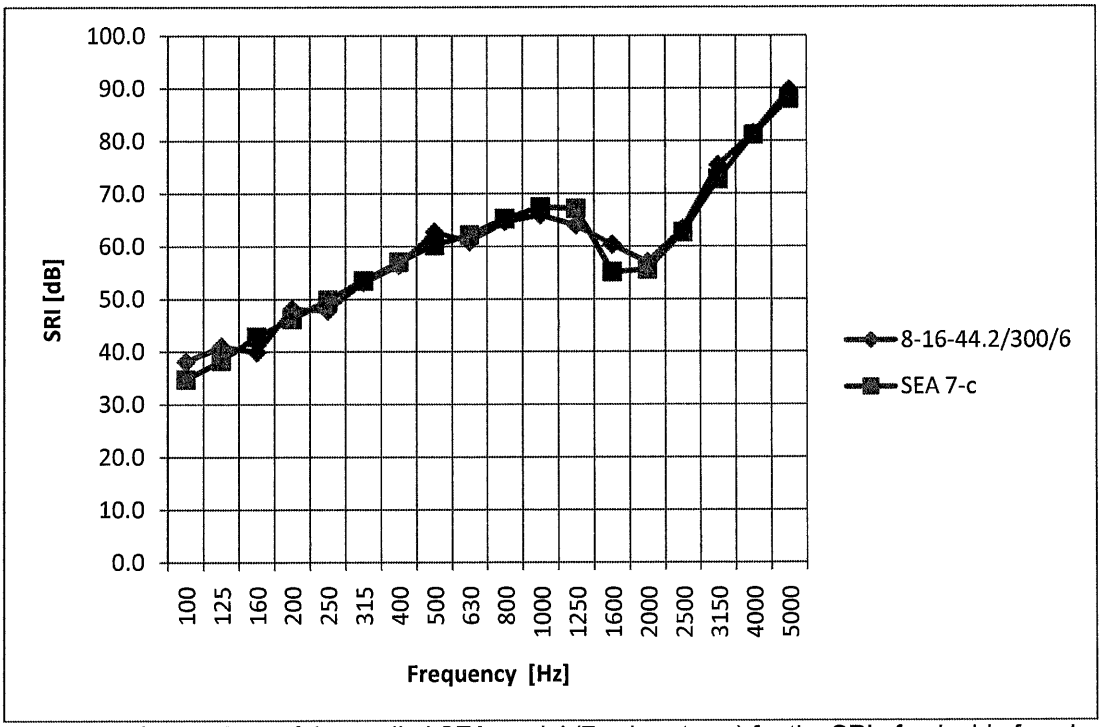

Figure 15: Comparison of the studied SEA model (7 subsystems) for the SRI of a double façade system with experimental result

4 STATISTICAL ERROR DESCRIPTION

4.1 Methods to compare the models used

The practical calculation work of the SRI was done using spreadsheet software, into which the studied SEA model was programmed. The SRI results are presented in 1/3 octave bands in the building acoustics range of 100 Hz to 5000 Hz. The validation of the models gives the accuracy of the models by comparing it to the experimental results and models can be compared with each other. The validation is done using the experimental data and several prediction error parameters [5].

The prediction error, E(f), is defined as the difference between the predicted and measured SRI at a specific frequency f:

$$E(f) = SRI_{pred}(f) - SRI_{meas}(f)$$

The prediction error $|E_n(f)|_{mean}$ for experiment n, is the averaged absolute value prediction error over 16 1/3 octave frequency bands:

$$|E_n(f)|_{mean} = \frac{1}{16} \sum_{f=100Hz}^{3150Hz} |E(f)|$$

The prediction error $|E(f)|_{mean}$ for frequency band f, is the averaged absolute value prediction error over 16 experiments:

$$|E(f)|_{mean} = \frac{1}{16} \sum_{n=1}^{16} |E_n(f)|$$

The average prediction error of the model averaged over 16 experiments and averaged over the 16 1/3 octave frequency bands:

$$< E(MODEL) >= \frac{1}{16}\sum_{n=1}^{16}|E_n(f)|_{mean} = \frac{1}{16}\sum_{f=100Hz}^{3150Hz}|E(f)|_{mean}$$

The average prediction error of the model gives the absolute frequency averaged deviation of the model in comparison to the experimental values, averaged over the total amount of experiments. The higher this value, the lower the accuracy of the model will be. The lower this value, the better the accuracy of the model to predict the SRI of a DGF system will be.
The error prediction of R_w for a model for experiment n is:

$$E(R_wMODEL) = (R_w)_{pred,n} - (R_w)_n$$

The average prediction error of R_w for a model and for 16 experiments used in the validation process is calculated by:

$$< E(R_wMODEL) >= \frac{1}{16}\sum_{n=1}^{16}\left|(R_w)_{pred,n} - (R_w)_n\right|$$

Where $(R_w)_n$ is the calculated R_w value of experiment n and $(R_w)_{pred,n}$ is the predicted R_w according to a model.
The model is considered acceptable when the average prediction error of the model or the average prediction error of R_w is below 5 dB. The model is considered good when the average prediction error of the model or the average prediction error of R_w is below 3 dB and it is considered very good when they are below 2 dB.
NOTE1: The prediction error $|E(f)|_{mean}$ is averaged over just 16 1/3 octave frequency bands (100Hz-3150Hz), as the measurements have shown that the measured SRI at 4000Hz and 5000 Hz gives underestimations of the real values due to laboratory limits. In order to be consistent for all measurements the 4000Hz and 5000Hz bands were omitted for the averaging process.
NOTE2: The prediction error $|E(f)|_{mean}$ is averaged taking into account the absolute value of the prediction error E(f). Using the prediction errors taking into account the sign of the values would yield a better than would be expected.
NOTE3: The value of R_w is mostly based on the performance at low frequencies. Therefore the prediction error $|E(f)|_{mean}$ is complementary because it considers all frequency bands equally.

4.2 Prediction errors SEA model

Figures 16 and 17 show the spectral prediction error and the prediction error for each experiment according to paragraph 4.1.

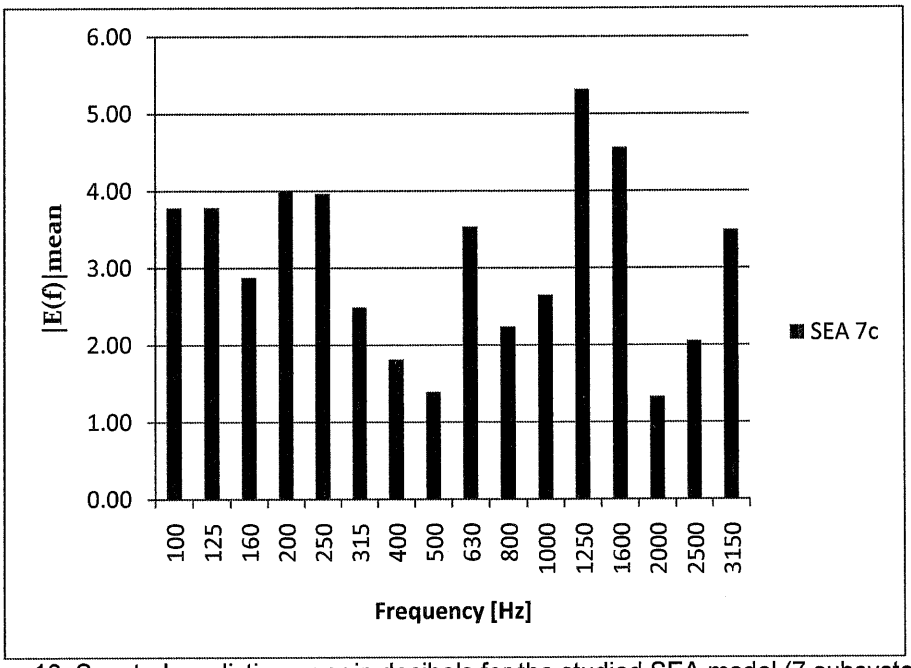

Figure 16: Spectral prediction error in decibels for the studied SEA model (7 subsystems)

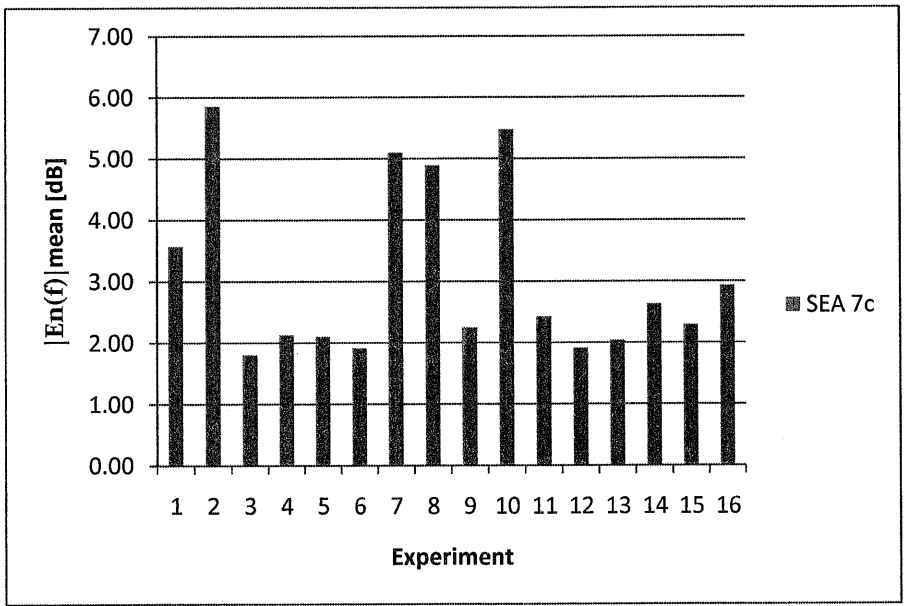

Figure 17: Prediction error per experiment in decibels for the studied SEA model (7 subsystems)

In table 3 the average prediction error of the model and R_w is given for different calculation models: the empirical model of Sharp [13], the SEA model using five subsystems according to Price & Crocker [12] and the SEA model using seven subsystems of the actual paper. From this table can be concluded that the best model is the model of the actual study using seven subsystems.

Looking at the single value for the sound reduction index, the average prediction error of R_w for the SEA model using seven subsystems is below 2 dB (table 3). According to Hongisto [5], this model reveals to be very good.
Looking spectrally at the sound reduction index, the average prediction error of this model is approximately 3 dB (table 3), revealing it to be a good model.

Table 3: Average prediction error of the model <E(MODEL)>, standard deviation s and <E(R_wMODEL)>

MODEL	<E(MODEL)> [dB]	s [dB]	<E(R_wMODEL)> [dB]
Sharp	13.40	3.4	12.25
Price & Crocker (SEA 5c)	6.28	2.5	13.12
SEA 7c	3.08	1.2	1.50

5 CONCLUSIONS

In this paper a SEA model using 7 subsystems has been presented to calculate the sound reduction index of a double façade system, consisting of three glass panels in total. The analysis predicts the effects of variation in panel damping and panel spacing on the transmission loss with very good accuracy. The calculation is quick and accurate, which is important for the acoustic assessment of double façade systems.
The use of the critical frequencies for all subsystems was derived from the measurements on these subsystems. The coupling loss factor between the two single glass panes connected by a spacer (i.e. the double glazing), was inserted in the studied SEA model by using the experimental values for the loss factors of the double glazing mounted in the aperture of the laboratory test wall. For the absorption coefficient in the cavity (subsystem 3 and 5), Brekke's values for normal incidence were used [2]. The use of a diffuse or a field incidence did not give important differences in the calculated SRI (less than 2 dB per frequency band).
The agreement with the experimental data revealed to be good to very good, with an average prediction error of the single value sound reduction index of 1.5 dB and an average prediction error of the model of 3 dB.
Further research will focus on the use of other materials than glass and the impact of the dimensions of the elements.

6 REFERENCES

[1] Blasco M. (2004) Actieve en Interactieve Dubbelschalige Glasgevels - Dubbele Gevels, TU Delft, The Netherlands

[2] Brekke A. – Calculation Methods for the Transmission Loss of Single, Double and Triple Partitions – Applied Acoustics 14 (1981) 225-240

[3] Craik R.J.M.– Non-Resonant Sound Transmission through Double Walls using Statistical Energy Analysis – Applied Acoustics 64 (2003) 325-341

[4] Fahy F., Gardonio P. (2007) Sound and Structural Vibration second edition, University of Southampton, UK

[5] Hongisto, V. (2006) Sound Insulation of Double Panels – Comparison of existing prediction models. Acta Acustica vol 92 (2006) 61-78

[6] Hopkins C.- Sound Insulation 1st edition – UK 2007

[7] London A. - Transmission of Reverberant Sound through Double Walls - J. Acoust. Soc. Am. Volume (22) Issue 2 270-279 (1950)

[8] Maidanik G.- Response of Ribbed Panels to Reverberant Acoustic Fields - J. Acoust. Soc. Am. (34) Issue 6 809-826 (1962)

[9] Norton M., Karczub D.– Fundamentals of Noise and Vibration Analysis for Engineers 2nd edition – Cambridge University Press – UK 2003

[10] Permasteelisa Group (1998) Architectural Envelopes and Blue Technology – M.I.T. Boston (USA)

[11] Permasteelisa Group (2003) Architectural Envelopes – fifth edition

[12] Price A.J., Crocker M.J.(1970) Sound transmission through double panels using statistical energy analysis. J.Acoust. Soc. Am. 47 p683-693

[13] Sharp B.H. - Prediction methods for the sound transmission of building elements. Noise Con. Eng. J. 11 (1978), p53-63

[14] Vermeir, G. (2000) Hogere Cursus Akoestiek-Bouwakoestiek. K.U.Leuven Applied Sciences Department.

[15] Vermeir, G. Roelens, A. Van Dommelen, H. (2005). Thesis: "Geluidisolatie van vensterramen en de invloed van raamkaders". KULeuven, Belgium.

[16] EN 12354-1 (2000) Building acoustics - Estimation of acoustic performance of buildings from the performance of elements - Part 1: Airborne sound insulation between rooms

[17] ISO 140-3 (1995) Acoustics - Measurement of sound insulation in buildings and of building elements -- Part 3: Laboratory measurements of airborne sound insulation of building elements

[18] ISO 3382 (1997) Acoustics - Measurement of the reverberation time of rooms with reference to other acoustical parameters